hardly degraded once incorporated into the sediments.

Conclusion

Incubation experiments of untreated domestic waste showed that the isomeric composition of LABs changes systematically due to microbial degradation. An I/E-degradation diagram (I/E ratio versus the extent of degradation of LABs) is proposed as an indicator of the degree of LAB degradation. By use of the I/E-degradation diagram, it was estimated that 55% of LABs entering the aquatic environment of Tokyo remain in the sediments without biodegradation.

Literature Cited

(1) Ishiwatari, R.; Takada, H.; Yun, S.-J.; Matsumoto, E. *Nature (London)* **1983**, *301*, 599-600.
(2) Takada, H.; Ishiwatari, R.; Yun, S.-J. *Jpn. J. Water Pollut. Res.* **1984**, *7*, 172-181.
(3) Takada, H.; Ishiwatari, R. *Environ. Sci. Technol.* **1987**, *21*, 875-883.
(4) Eganhouse, R. P.; Blumfield, D. L.; Kaplan, I. R. *Environ. Sci. Technol.* **1983**, *17*, 523-530.
(5) Albaigés, J.; Farrán, A.; Soler, M.; Gallifa, A.; Martin, P. *Mar. Environ. Res.* **1987**, *22*, 1-18.
(6) Eganhouse, R. P.; Ruth, E. C.; Kaplan, I. R. *Anal. Chem.* **1983**, *55*, 2120-2126.
(7) Eganhouse, R. P.; Kaplan, I. R. *Mar. Chem.* **1988**, *24*, 163-191.
(8) Valls, M.; Bayona, J. M.; Albaigés, J. *Nature* **1989**, *337*, 722-724.
(9) Eganhouse, R. P.; Olaguer, D. P.; Gould, B. R.; Phinney, C. S. *Mar. Environ. Res.* **1988**, *25*, 1-22.
(10) Vivian, C. M. G. *Sci. Total Environ.* **1986**, *53*, 5-40.
(11) *Sewerage in Tokyo*; Sewerage Bureau of Tokyo Metropolitan Government: Tokyo, Japan, 1985.
(12) Takada, H.; Ishiwatari, R. *J. Chromatogr.* **1985**, *346*, 281-290.
(13) Nakae, A.; Tsuji, K.; Yamanaka, M. *Anal. Chem.* **1980**, *52*, 2275-2277.
(14) Nakae, A.; Tsuji, K.; Yamanaka, M. *Anal. Chem.* **1981**, *53*, 1818-1821.
(15) Bayona, J. M.; Albaigés, J.; Solanas, A. M.; Grifoll, M. *Chemosphere* **1986**, *15*, 595-598.
(16) Matsumoto, E. *Chikyu Kagaku (Nippon Chikyu Kagakkai)* **1983**, *17*, 27-32.

Received for review June 9, 1988. Revised manuscript received March 2, 1989. Accepted August 3, 1989. This work was partly supported by the Ministry of Education, Science and Culture, Japan (Grants 58030062, 59030064, 6030069, and 61030005) and The Tokyu Foundation for the Better Environment (Grant 5724).

Transformations of Selenium As Affected by Sediment Oxidation–Reduction Potential and pH

Patrick H. Masscheleyn,* Ronald D. Delaune, and William H. Patrick, Jr.

Laboratory for Wetland Soils and Sediments, Center for Wetland Resources, Louisiana State University, Baton Rouge, Louisiana 70803-7511

■ The influence of E_h and pH on selenium solubility, speciation, and volatilization was studied. Kesterson Reservoir sediments contaminated with selenium were incubated under controlled redox (-200, 0, 200, and 450 mV) and pH (6.5, natural, 8.5, and 9) conditions. Under reduced conditions selenium solubility was low and controlled by an iron selenide phase. Se(-II,0) comprised 80–100% of the total soluble selenium. Upon oxidation dissolved selenium concentrations increased. The oxidation of Se(-II,0) to selenite was rapid and occurred immediately after the oxidation of iron. Above 200 mV selenite slowly oxidized to selenate. Under oxidized conditions (450 mV) selenium solubility reached a maximum. Selenate was the predominant dissolved species present, constituting 95% at higher pH's (8.9, 9) to 75% at lower pH's (7.5, 6.5) of the total soluble selenium at 450 mV. Biomethylation of selenium occurred only under oxidized conditions. Redox potential and pH are key factors in the biogeochemistry of selenium.

Introduction

The discovery of toxic concentrations of selenium in evaporation ponds of the Kesterson National Wildlife Refuge, located in the Western part of California's San Joaquin Valley, has led to an increasing interest in the biogeochemistry of selenium in recent years.

The chemistry of selenium is complicated since it can exist in four different oxidation states, selenide (Se(-II)), elemental Se (Se(0)), selenite (Se(IV)), and selenate (Se (VI)), and as a variety of organic compounds. The major features of selenium biogeochemistry affecting its movement and toxicity are associated with changes in its oxidation state and the resulting differences in chemical properties of these various chemical forms. Adsorption and mobility of the selenite and selenate species have been studied extensively during the past few years (*1–7*). Briefly, conditions that favor the mobility of selenium with respect to adsorption are alkaline pH, oxidizing conditions, and high concentrations of additional anions.

Although the importance of the redox status in the study of selenium biogeochemistry is evident, few studies have investigated the effects of changes in oxidation–reduction potential on the transformations of selenium species in soils and sediments. Geering et al. (*8*) constructed an E_h–pH diagram and theoretically investigated selenium transformations as affected by pH and E_h. In a more recent paper, Elrashidi et al. (*9*) used thermodynamic data to develop equilibria reactions and constants for selenium minerals and solution species that relate to soils. Based upon thermodynamics, they reported metal–selenite and in particular metal–selenate minerals to be too soluble to persist in soils. At low redox potentials, however, elemental Se or a metal–selenide could control Se solubility.

We developed a laboratory experiment that allowed us to study selenium transformations under controlled redox and pH conditions. In this paper we describe the critical redox levels at which selenium transformations in contaminated Kesterson Reservoir sediments occurred and report the influence of redox and pH on selenium speciation, solubility, and volatilization.

Experimental Section

Sediments. Selenium-contaminated soils (further called sediments) of the Kesterson Reservoir in California were

0013-936X/89/0924-0091$02.50/0

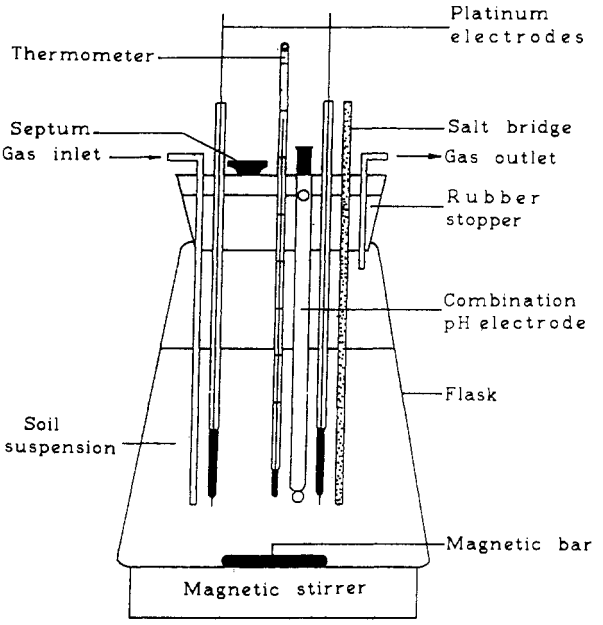

Figure 1. Schematic of experimental setup used for pH and redox control of the sediment suspensions.

collected at the northeast side of pond no. 2, approximately 30 m from the levee. The sediment was transported to the laboratory in tightly closed plastic containers. Upon arrival, the sediments were homogenized under an argon atmosphere and stored in closed 4-L polyethylene flasks until use.

Incubation Apparatus. The sediments were incubated in laboratory microcosms at various redox–pH conditions by using a modification of the redox control system developed by Patrick et al. (*10*) (Figure 1). In this system, the suspension pH is continuously measured and manually adjusted by additions of 4 M HCl or NaOH, daily, or as required to bring the pH to the desired value. The redox potential was maintained at a preselected potential automatically. Platinum electrodes in the suspension were connected to a millivolt meter to give continuous measurement of the redox potential of the sediment–water suspension. The recorder output of the millivolt meter was in turn connected to a meter relay that activated an air pump. Whenever the redox potential dropped below the desired potential, a small amount of air was pumped into the system to maintian the desired redox potential. This system of regulating redox potential with air input works because, in the absence of oxygen, chemical and especially microbial processes cause the redox potential to decrease. The flasks were continuously purged with oxygen-free argon gas. Argon gas was effective in purging excess air at the end of the aeration cycle and in preventing a buildup of gaseous decomposition products such as carbon dioxide and hydrogen sulfide. Using this system, we could maintain the desired redox potential within ±20 mV. The outflow gas passed out the incubation apparatus into a 10-mL concentrated HNO_3 solution followed by a water trap. Nitric acid has been reported to retain volatile selenium compounds from soils (*11*).

Experiments. In experiment one, the critical redox levels where selenium transformations occur were determined. Suspensions of the strongly reduced sediments were incubated (at 28 ± 2 °C) in the microcosms for 6 h before adjusting redox levels. Suspensions were prepared by mixing an amount of sediment equivalent to 200 g of dry weight with distilled water so that the final sediment water ratio was 1 to 7. Four incubations were performed each at a different E_h; −200, 0, 200, and 450 mV. The experiment was run in duplicate. The microcosms were sampled at a 5-day interval over a 3-week period. The pH was monitored and recorded.

In experiment two, similar sediment suspensions were equilibrated under controlled redox and pH conditions. The following redox–pH combinations were used: redox −200, 0, 200, and 450 mV; pH 6.5, natural, 8.5, and 9. Natural (uncontrolled) pH values after a 28-day incubation period were 7.5 for 450 mV, 7.8 for 200 mV, 7.9 for 0 mV, and 8.1 for −200 mV. Microcosms were sampled after 28 days of incubation. Incubations were run in duplicate.

A sediment suspension aliquot was withdrawn, centrifuged [20 min at 7000 rpm (31*g*), Sorvall GSA-400 rotor, Du Pont CO., Wilmington, DE] and filtered through a 0.45-μM micropore filter, under an inert argon atmosphere for reduced treatments (*12*). Five dissolved selenium species were identified in the water extract.

In order to better validate E_h measurements in the systems we also measured the NO_3/NH_4, soluble Mn (Mn(II)), soluble Fe (Fe(II)), and the SO_4/S redox species. Other major cations (Ca, Mg, K, Na, Al), metals (Cu, Zn, Cd, Pb, Ni), and chlorides were also determined.

Analysis. Selenium species (Se(IV), Se(VI), Se(−II,0), dimethyl selenide (DMSe), and oxidized methylated Se compounds (Ox·MSe) in the water extracts were determined with a hydride generation/trapping/detection apparatus. The system was similar to that described by Cooke and Bruland (*13*). It included a helium-purged glass stripping vessel, a glass U tube immersed in an isopropyl alcohol–ice bath, a glass U tube immersed in liquid nitrogen, and an atomic absorption spectrophotometer (Perkin-Elmer 360) fitted with a flame in tube burner. A slightly longer hydride trap (40 cm) was used. Column packing material was found not necessary to separate methylated selenium compounds from selenium hydride. The output was recorded on a strip chart recorder and peak heights were used to calculate concentrations. Absorbance was found to be linear over the range 0–150 ng of selenium (amount placed in the hydride generator) with a sensitivity of 0.0045 absorbance units ng^{-1} of Se and a detection limit of 5 ng of Se.

Extracts were analyzed for selenium species within 10 h after sampling. A 10-mL aliquot of the extract was purged with He for the determination of volatile dimethyl selenide. Aliquots that had been previously stripped of volatile methylated compounds were then analyzed for selenite and dissolved oxidized methylated selenium compounds (*13*). Other aliquots were analyzed for (selenate + selenite), after reduction of Se(VI) to Se(IV) in 6 M HCl (*14*), and for total selenium by a modification (*15*) of the method described by Presser and Barnes (*16*). Sulfanilamide was used to eliminate possible nitrite interference in the determination of selenium (*17*). The selenate was calculated as the difference between the (selenate + selenite) and the selenite analysis. The difference between the total Se content and the (selenate + selenite) fraction is the Se(−II,0) fraction. The maximum sample volume analyzed for inorganic selenium species was 5 mL, which gave a detection limit of 1 μg of Se L^{-1} or 7 μg of Se kg^{-1} of dry sediment. Due to the small sample volume analyzed (normally between 0.5 and 2 mL), no interferences in the analysis of selenium species by dissolved organic carbon (*15*, *18*) were found. Several samples were analyzed by the standard addition technique. The relative precision of the technique was the same as reported by Cooke and Bruland (*13*): 5% for selenium species that were determined directly and ~10% for the species determined by difference. For the quantification of the volatilized selenium com-

Table I. Concentration of Soluble Redox Species and Ca during a 20-Day Incubation Period at −200 mV

	concn, mg kg^{-1} of dry sediment							concn, $\mu g\ kg^{-1}$	
day	NH_4 N	NO_3 N	Mn	Fe	S(−II)	SO_4 S	Ca	Se(−II,0)	Se(IV)
2	212[a]	<2.00[c]	5.74	7.73	65	2905	934	21	<7[c]
	±11[b]		±0.20	±0.67	±9	±770	±229	±7	
7	241	<2.00	4.22	7.90	74	2919	903	56	<7
	±3		±1.48	±1.68	±20	±679	±168	±28	
12	264	<2.00	5.47	7.95	64	3052	931	42	<7
	±12		±0.56	±1.72	±20	±546	±204	±23	
20	259	<2.00	4.55	7.85	70	3395	1091	84	<7
	±6		±1.32	±0.76	±22	±1021	±165	±15	

[a] Mean of duplicate incubations. [b] Standard deviations. [c] Detection limit.

Table II. Concentration of Soluble Redox Species and Ca during a 20-Day Incubation Period at 0 mV

	concn, mg kg^{-1} of dry sediment							concn, $\mu g\ kg^{-1}$	
day	NH_4 N	NO_3 N	Mn	Fe	S(−II)	SO_4 S	Ca	Se(−II,0)	Se(IV)
2	258[a]	<2.00[c]	4.22	7.95	50	3402	1068	44	<7[c]
	±8[b]		±0.37	±1.01	±3	±98	±230	±10	
7	229	<2.00	4.23	6.90	42	3556	1165	42	<7
	±9		±1.34	±1.71	±15	±826	±285	±2	
12	246	<2.00	5.18	8.00	45	3801	1400	72	<7
	±12		±1.57	±1.90	±15	±714	±290	±14	
20	259	<2.00	7.21	0.55	3	5056	2305	35	259
	±26		±0.82	±0.25	±3	±1174	±475	±7	±103

[a] Mean of duplicate incubations. [b] Standard deviation. [c] Detection limit.

pounds, the HNO_3 solutions were carefully taken to near dryness, 40 mL of 4 M HCl was added, and the solutions were treated as for (selenite + selenate) analysis.

Ammonium and nitrate were determined by the Kjeldahl distillation technique. Metals and major cations in solution were analyzed with a Jarrel Ash ICP, and a Dionex Ion Chromatograph was used for chloride and sulfate analysis. EPA reference standards were analyzed to check the preformance of the ICP. Sulfide was measured by an ion-specific Ag/S electrode in an anoxic buffer solution (sulfide electrode operating instruments; Lazar Research Laboratories, Los Angeles, CA). Due to the limited sensitivity of the electrodes, these analyses are probably less accurate.

Total Se in the sediment was determined by the prewetting digestion procedure as described by Fujii et al. (*15*).

The loss on ignition method (*19*) was used to estimate the organic matter content of the sediment.

X-ray diffraction (Cu Kα radiation) of bulk powder samples was used to study the mineralogy of reduced and oxidized sediment.

Results and Discussion

Critical Redox Potentials for Selenium Transformations. The sediments from the Kesterson Reservoir were extensively anaerobic and characterized by a high pH (8.1), an organic matter content of 5.2%, and a dark grayish color due to the large concentration of iron monosulfides. Presser and Barnes (*16*) reported the presence of thenardite (Na_2SO_4) in Kesterson reservoir sediments. Our X-ray diffraction patterns showed the presence of a large amount of calcite and some pyrite in the reduced sediments. The sediment had a total Se content of 9.06 ± 2.40 mg kg^{-1} (n = 8) of dry sediment.

The critical redox potentials at which selenium transformations occurred were determined (experiment one). Results for a 3-week incubation study at −200 (PE = E_h/59.16) and 0 mV are given in Tables I and II. When incubated at −200 mV (pH 8.1), the solubility of selenium was very low and Se(−II,0) was the only detectable form (Table I). At −200 mV nitrogen, manganese, and iron were present in a reduced form. Sulfide concentrations up to 74 mg kg^{-1} of dry sediment were measured. High chloride, sodium, and sulfate concentrations (approximately 4200, 3750, and 3400 mg kg^{-1} of dry sediment, respectively) were due to the solubility of salts like Na_2SO_4 and NaCl. As the incubation time progressed, concentrations of dissolved Na and Cl remained constant in both reduced and oxidized experiments, suggesting the independence of their solubility from oxidation–reduction reactions. Soluble Cu, Zn, Cd, Pb, and Ni were less than 1 mg kg^{-1} of dry sediment.

Oxidation of Se(−II,0) to Se(IV) occurred at an E_h of approximately 0 mV (Table II). For the first 14 days total soluble selenium concentrations and forms at 0 mV (pH 7.9) were comparable with those reported for the incubation at −200 mV. However, after approximately 2 weeks the color of the suspension changed gradually from dark grayish to light brown due to the formation of iron oxides. Levels of dissolved iron and sulfides decreased and the sulfate concentration increased sharply, illustrating the oxidation of the iron sulfides. The concurrent increase of the calcium concentration (Table II) is somewhat ambiguous. It could result from the dissolution of gypsum ($CaSO_4 \cdot 2H_2O$) or anhydrite ($CaSO_4$)

$$CaSO_4 \cdot 2H_2O = Ca^{2+} + SO_4^{2-} + 2H_2O \quad (1)$$

or it could result from the oxidation of an iron sulfide (pyrite or an iron monosulfide) and reaction with calcite:

$$FeS_2 + 3.75O_2 + 3.5H_2O = Fe(OH)_3 + 4H^+ + 2SO_4^{2-} \quad (2)$$

$$4H^+ + 2CaCO_3 = 2Ca^{2+} + 2H_2CO_3 \quad (3)$$

It is very difficult to distinguish [except perhaps by study of sulfur isotopes (*20*)] between these alternatives without investigation of the solid phases involved. Mineral identification by X-ray diffraction clearly showed the absence of gypsum and the presence of large amounts of both iron sulfides and calcite in the reduced sediments. Therefore the reactions described in eq 2 and 3 are responsible for

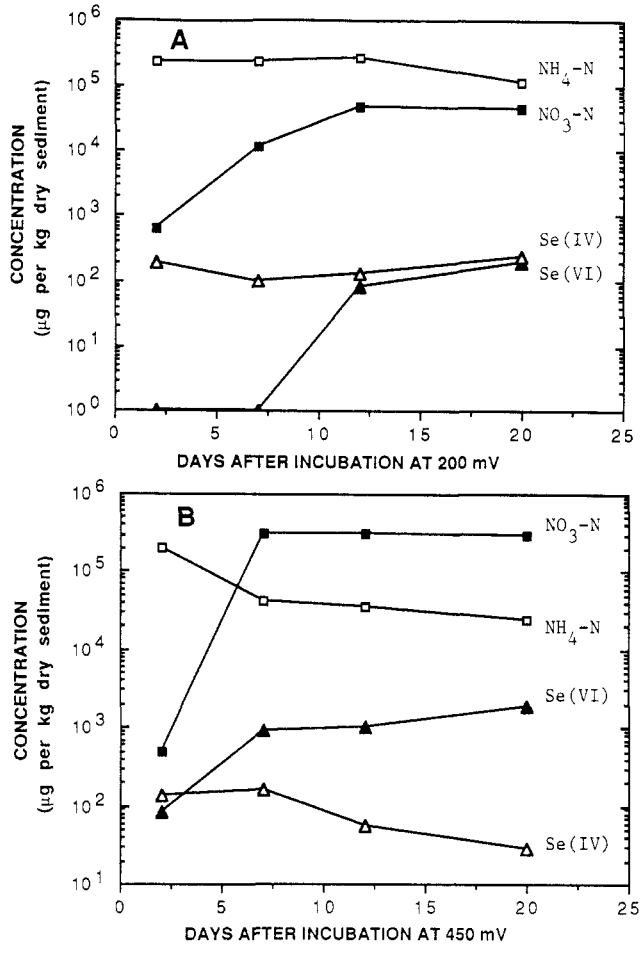

Figure 2. Ammonium/nitrate and selenite/selenate transformations during a 20-day incubation period. (A) at 200 mV. (B) at 450 mV.

the increase of Ca concentration in our experiments. A large part of the alkalinity formed is lost to the atmosphere as CO_2.

Analysis of variance [PROC GLM procedure of the Statistical Analysis System (*21*)], comparing the solubility of redox species and calcium at −200 vs 0 mV, supports the interpretations made above. Concentrations of soluble redox species and Ca were not significantly different between the two redox levels studied. However, significant ($P < 0.05$) differences were found for the dissolved concentrations of Fe, S(−II), Ca, and Se(IV) between the different sampling times. There also was a significant interaction ($P < 0.05$) between the days after incubation and the E_h for these elements. As can be implied from Tables I and II, the interaction (day 20, −200 vs 0 mV) can be interpreted as the oxidation of iron sulfides, the consequent release and oxidation of Se(−II,0) to selenite, and the reactions described in eq 2 and 3.

The dominant selenium species found at 200 and 450 mV are shown in Figure 2. The transformation of selenite to selenate began at a redox potential of approximately 200 mV (pH was 7.7 at end of incubation) and occurred at values corresponding with nitrification and denitrification. Low concentrations of dissolved Mn (0.17 ± 0.08 mg kg^{-1}), Fe (0.87 ± 0.36 mg kg^{-1}), and S(−II) (<0.02 mg kg^{-1}) were typical for the oxidized sediment. Concentrations of Ca and SO_4 S at the end of the incubation period were 2710 ± 212 and 4780 ± 590 mg kg^{-1} of dry sediment, respectively. When incubated at 450 mV, the oxidation of ammonium to nitrate and selenite to selenate was evident after 2 days of incubation (Figure 2B). Over time almost all selenite was oxidized and selenate became the

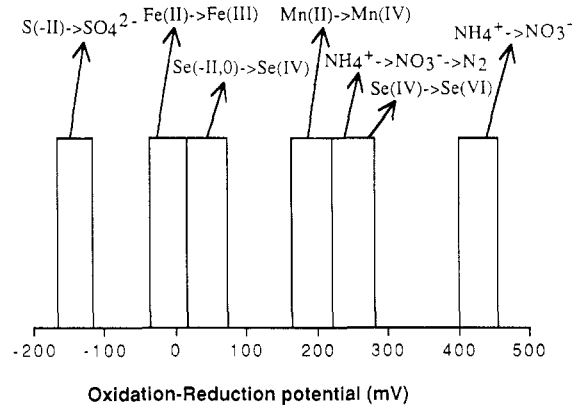

Figure 3. Sequential oxidation of several redox systems in Kesterson Reservoir Sediments.

Table III. Solubility Products at 25 °C and 10^5 Pa

mineral	reaction products	−log K_{sp}	ref
α-$Fe_{0.95}S$ (pyrrhotite)	$0.85Fe^{2+}$ + $0.10Fe^{3+}$ + S^{2-}	18.74	23
α-FeS (troilite)	Fe^{2+} + S^{2-}	16.21	23
FeS_2 (pyrite)	Fe^{2+} + S_2^{2-}	26.93	23
FeS_2 (markasite)	Fe^{2+} + S_2^{2-}	26.23	23
FeSe (achavalite)	Fe^{2+} + Se^{2-}	26.00	9

dominant selenium species in solution. At the end of the incubation the dissolved concentrations of the other redox species (mg kg^{-1} of dry sediment) were as follows: Mn, 0.08 ± 0.05; Fe, 0.61 ± 0.48; S(−II), <0.02. During the incubation the pH dropped from 8.1 to 7.5 and soluble SO_4 S and Ca concentrations rose to 5159 ± 903 and 3160 ± 480 mg kg^{-1}, respectively.

Figure 3 summarizes the order of various inorganic oxidation–reduction reactions for the Kesterson Reservoir sediments. The same sequence was found in preliminary studies (results not shown), where transformations of added selenite were determined in Mississippi River sediments under controlled redox conditions. Data presented indicate that the oxidation and chemical weathering of iron sulfides leads to increases in soluble selenium species. The released Se(−II,0) is quickly oxidized to selenite. We also found that the oxidation of selenite to selenate occurred at a considerable higher E_h than the sulfide to sulfate oxidation. The oxidation rate of selenite to selenate is rather slow and is a function of the redox potential. Selenate was detected only when nitrate was present. From our experiments, it is difficult to calculate exact transformation rates because adsorption–desorption reactions occur simultaneously with the oxidation reactions.

From our study it is clear that selenium solubility increases with increased redox potential. It also seems that the chemistry of selenium under reduced conditions is closely related to that of iron. Recently Elrashidi et al. (*9*), using thermodynamic data to develop chemical equilibria reactions and constants of selenium in soils, also reported very low solubilities of selenides under reduced conditions. When an iron sulfide mineral forms in natural waters or sediments, the first phase to precipitate is usually an unstable monosulfide (*22*). Solubility products of iron monoselenide and sulfides are given in Table III. If we assume that selenide can substitute for sulfide in a solid solution phase, for example, troilite (Fe(S,Se)), then from the equilibrium reaction

$$FeS + Se^{2-} = FeSe + S^{2-} \quad (4)$$

with $\log K = \log (a_{FeSe}/a_{FeS}) + \log (a_{S^{2-}}/a_{Se^{2-}}) = 9.79$, it can be seen that even in the presence of high sulfide concen-

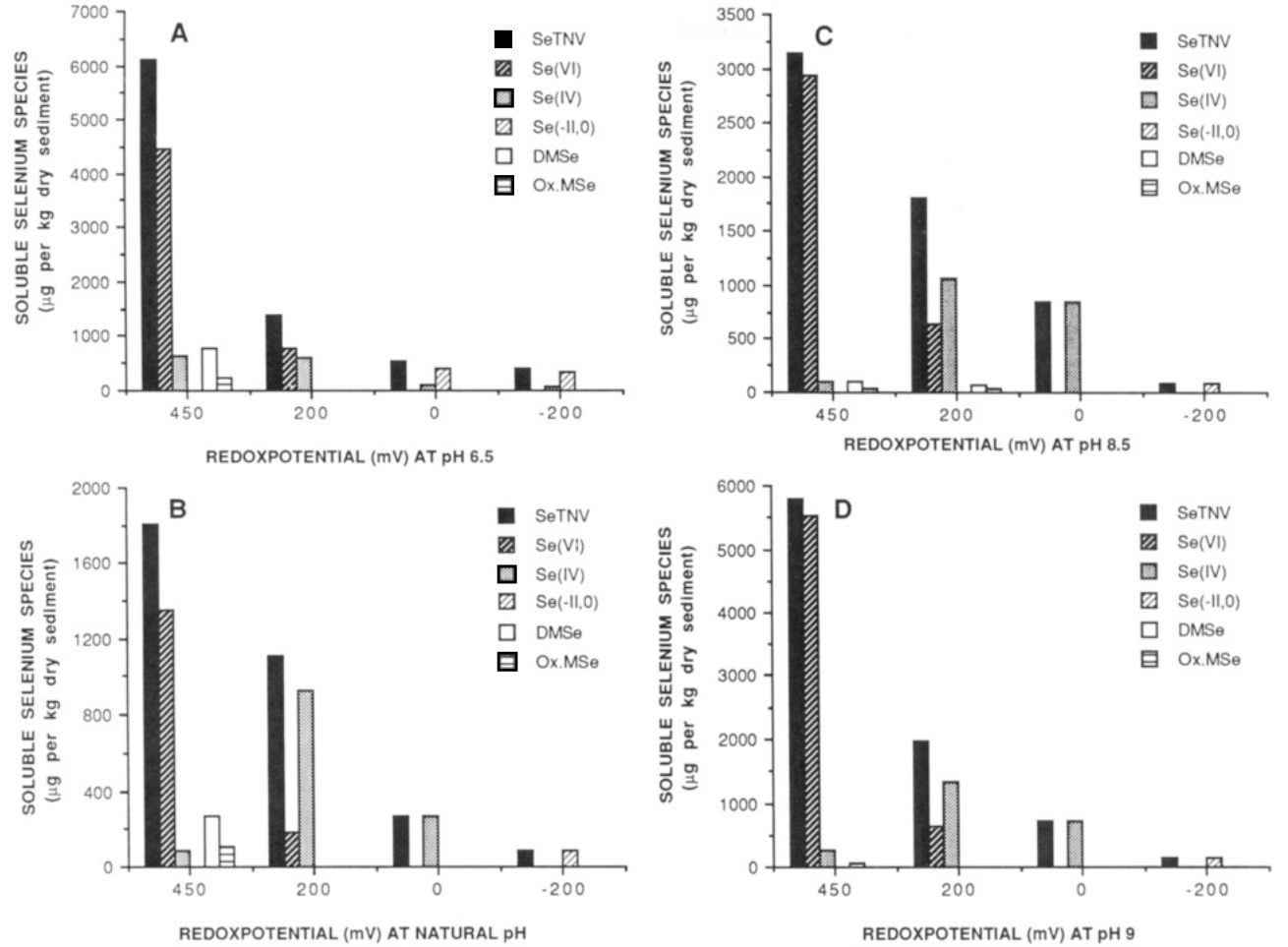

Figure 4. Distribution of soluble selenium species after a 28-day incubation period under controlled redox and pH conditions. (A) incubations at pH 6.5. (B) incubations at natural pH (7.5 for 450 mV, 7.8 for 200 mV, 7.9 for 0 mV, and 8.1 for −200 mV). (C) incubations at pH 8.5. (D) incubations at pH 9.

trations only a very small amount of selenide is needed in order to get supersaturation with respect to the iron selenide component in the solid solution. Over time monosulfides are generally oxidized to pyrite ($FeS + S^0 = FeS_2$) (*22*), and it is very likely that in the presence of elemental sulfur the reaction $FeSe + S^0 = FeSeS$ exists. Although the existence of such a compound has not been proven yet, it undoubtedly may exist in nature. Howard (*24*) summarized selenium geochemistry on an E_h–pH diagram and included a stability field for the mineral ferroselite ($FeSe_2$). The redox–pH conditions of the reduced Kesterson Reservoir sediments are in accordance with this stability field. In the presence of an excess elemental sulfur, ferroselite was found to be unstable with respect to pyrite. The released elemental selenium was thought to be incorporated in pyrite (*24*).

Influence of Redox Potential and pH on Selenium Solubility, Speciation, and Volatilization. The redox–pH chemistry of indigenous selenium in Kesterson Reservoir sediments in relation to its solubility and its distribution among the various chemical species was determined (experiment two). Figure 4 shows the species distribution of total soluble selenium after 4 weeks of incubation at four different redox levels (−200, 0, 200, and 450 mV) ranging from strongly reduced to well oxidized. Four suspension pH levels (6.5, natural, 8.5, and 9) were selected and maintained during the incubation period. Incubations at pH values lower than 6.5 led to a massive dissolution of $CaCO_3$ and the precipitation of $CaSO_4 \cdot 2H_2O$ and were therefore not included in this study. Total nonvolatile selenium (SeTNV) represents the sum of the inorganic (Se(−II,0), Se(IV), Se(VI)), and organic (DMSe and Ox·MSe) selenium compounds that was in solution at the time of sampling.

The selenium solubility strongly increased with increasing redox potential for all pH treatments. The pH had a major effect upon both the levels and chemical forms of dissolved selenium. In general, the selenium solubility was lowest in the incubations at natural pH. Both an increase or decrease in pH led to a higher amount of total soluble selenium. The highest total soluble selenium concentrations were found at a pH of 6.5. Up to 67% of the total Se present in the sediment was found to be soluble at the high redox level (450 mV). This was due to the higher solubility of the iron sulfides and the concurrent release of selenium into solution. The precipitation of Ca^{2+} and SO_4^{2-} as gypsum maintained the reactions in eq 2 and 3. Presser and Barnes (*16*) reported a small substitution of SeO_4^{2-} for SO_4^{2-} in gypsum precipitated from water samples of the Kesterson Reservoir. In our experiment we did not find evidence of precipitation of a $CaSeO_4$ or $CaSeO_3$ phase, although the formation of such highly soluble compounds is probably possible in conditions of a dry and hot climate. The increase in soluble selenium at pH values greater than 7.5 was significant only at 450 mV. Under the oxidized conditions (450 mV), 20–63% of the total Se present in the sediment was solubilized, depending on the pH. This increase can be explained by the decrease in adsorptive capacity of the soil, especially from the oxidized iron forms for selenite with increasing pH. The adsorption processes of selenite and selenate have been extensively studied in recent years

(*4–8*). It is generally accepted that selenite adsorption decreases with increasing pH in the range 4–9 and that selenate adsorption is minimal under most pH conditions. The oxidation of iron sulfides resulted in the formation of hydroxylated ferric oxides whose surfaces can adsorb selenite and to a much lesser extent selenate.

The species distribution of selenium identified in the present study is consistent with the stability field of Se species in theoretically derived E_h–pH diagrams (*6, 24, 25*). Selenate was the major dissolved species under highly oxidized conditions, constituting 95% at higher pH's (8.5, 9) to 75% at lower pH's (7.5, 6.5) of the SeTNV. The Se(–II,0) concentrations were below the detection limit at the high redox levels and the Se(IV) only became detectable at the lower pH levels. At 200 mV, the major part of the SeTNV (60–78%) was in the selenite form. When incubated at 0 mV, there seems to be a rapid oxidation of the Se(–II,0) to selenite since no Se(–II,0) could be detected. No oxidation of selenite to selenate occurred at 0 mV during the 4-week incubation period. In the reduced (–200 mV) treatment, Se(–II,0) comprised 80–100% of the SeTNV. Selenite was detected only at pH 6.5.

Dissolved DMSe and oxidized methylated selenium compounds were detected only in the aerobic incubations. DMSe comprised 15% of the SeTNV, while the Ox·MSe fraction made up to 5% of the SeTNV. Assimilation of selenite and reductive methylation have been proposed as first steps in the methylation pathway of selenium (*25, 26*). Cooke and Bruland (*13*) showed outgassing of selenium in the biologically active Kesterson Reservoir to be substantial. They suggested that the production of DMSe occurred by intra- and/or extracellular transformation of biogenically derived *Se*-methylselenomethionine. Although we found dissolved methylated selenium compounds only under aerobic conditions, selenium volatilization under anaerobic conditions has also been reported (*26–28*). It is important to note that in these studies very high selenium concentrations were added to the soil. In the experiment reported here, solubility of indigenous selenium was very low under the reduced conditions (Tables I and II). Contamination of the analytical-grade HNO_3 with selenium (up to 20 ng mL^{-1}), used to trap evolved selenium species, made it difficult to determine the exact amount of selenium volatilized. However, after making the appropriate corrections, we found selenium volatilization to be significant only at 200 and 450 mV. No evidence was found for selenium volatilization under reduced conditions in our experiments.

Conclusions

Sediment redox potential and pH were shown to control the speciation and solubility of selenium. At low redox levels selenium solubility was low and controlled by an iron selenide phase. Total soluble selenium concentrations substantially increased upon oxidation or increase in sediment redox potential. Under highly oxidized conditions, selenate became the major species in solution and soluble selenium concentrations reached a maximum. Dimethyl selenide and other dissolved methylated selenium compounds were detected only under oxidized conditions. Redox potential and pH exhibit a major impact on selenium speciation, solubility, and volatilization and are therefore of paramount importance in the study of selenium biogeochemistry.

Acknowledgments

We are grateful to the U.S. Geological Survey for collecting and providing the sediments used in this study and to Dr. M. Walthall for his help with the X-ray diffraction work.

Registry No. Se, 7782-49-2; NH_4^+, 14798-03-9; Mn, 7439-96-5; Fe, 7439-89-6; S, 7704-34-9; Ca, 7440-70-2; pyrrhotite, 1310-50-5; troilite, 1317-96-0; pyrite, 1309-36-0; markasite, 1317-66-4; achavalite, 38007-30-6.

Literature Cited

(1) Ahlrichs, J. S.; Hossner, L. R. *J. Environ. Qual.* **1987**, *16*, 95–98.
(2) Alemi, M. H.; Goldhamer, D. A.; Grismer, M. E.; Nielsen, D. R. *J. Environ. Qual.* **1988**, *17*, 613–618.
(3) Alemi, M. H.; Goldhamer, D. A.; Nielsen, D. R. *J. Environ. Qual.* **1988**, *17*, 603–613.
(4) Balistrieri, L. S.; Chao, T. T. *Soil Sci. Soc. Am. J.* **1987**, *51*, 1145–1151.
(5) Bar-Yosef, B.; Meek, D. *Soil Sci.* **1987**, *144*, 11–19.
(6) Neal, R. H.; Sposito, G.; Holtzclaw, K. M.; Traina, S. J. *Soil Sci. Soc. Am. J.* **1987**, *51*, 1161–1165.
(7) Neal, R. H.; Sposito, G.; Holtzclaw, K. M.; Traina, S. J. *Soil Sci. Soc. Am. J.* **1987**, *51*, 1165–1169.
(8) Geering, H. R.; Cary, E. E.; Jones, L. H.; Allaway, W. H. *Soil Sci. Soc. Am. J.* **1968**, *32*, 35–40.
(9) Elrashidi, M. A.; Adriano, D. C.; Workman, S. M.; Lindsay, W. L. *Soil Sci.* **1987**, *144*, 141–152.
(10) Patrick, W. H., Jr.; Williams, B. G.; Moraghan, J. T. *Soil Sci. Soc. Am. J.* **1981**, *37*, 331–332.
(11) Abu-Erreish, G. M.; Whitehead, E. I.; Olson, O. E. *Soil Sci. Soc. Am. J.* **1968**, *106*, 415–420.
(12) Patrick, W. H., Jr.; Henderson, R. E. *Soil Sci. Soc. Am. J.* **1981**, *45*, 855–859.
(13) Cooke, T. D.; Bruland, K. W. *Environ. Sci. Technol.* **1987**, *21*, 1214–1219.
(14) Brimmer, S. P.; Fawcett, R. W.; Kulhavy, K. A. *Anal. Chem.* **1987**, *59*, 1470–1471.
(15) Fujii, R.; Deverel, S. J.; Hatfield, D. B. *Soil Sci. Soc. Am. J.* **1988**, *52*, 1274–1283.
(16) Presser, T. S.; Barnes, I. *Water Res. Invest. Rep.* (U.S. Geol. Surv.) **1984**, *84*–4122.
(17) Cutter, G. A. *Anal. Chim. Acta* **1983**, *149*, 391–394.
(18) Roden, R. D.; Tallman, D. E. *Anal. Chem.* **1982**, *54*, 307–309.
(19) Davies, B. A. *Soil Sci. Soc. Am. J.* **1974**, *38*, 150–151.
(20) Drever, J. I. *The Geochemistry of Natural Waters*, 2nd ed.; Prentice Hall: Englewood Cliffs, NJ, 1988; Chapter 11.
(21) SAS Institute, Inc. *SAS User's Guide*; SAS Institute, Inc.: Cary, NC, 1985.
(22) Berner, R. A. *Am. J. Sci.* **1970**, *268*, 1–23.
(23) Lindsay, W. L. *Chemical Equilibria in Soils*; Wiley: New York, 1979; Chapter 17.
(24) Howard, J. H., III, *Geochim. Cosmochim. Acta* **1977**, *41*, 1665–1678.
(25) Coleman, R. G.; Delevaux, M. *Econ. Geol.* **1957**, *52*, 499–501.
(26) Doran, J. W.; Alexander, M. *Soil Sci. Soc. Am. J.* **1976**, *40*, 687–690.
(27) Challenger, F. *Adv. Enzymol.* **1951**, *12*, 432–486.
(28) Reamer, D. C.; Zoller, W. H. *Science (Washington, D.C.)* **1980**, *208*, 500–502.

Received for review March 3, 1989. Accepted August 25, 1989.